

Influence of Ag additions on the activation energy for the reverse eutectoid reaction in Cu–Al alloys

T. M. Carvalho · A. T. Adorno · A. G. Magdalena ·
R. A. G. Silva

CBRATEC7 Conference Special Issue
© Akadémiai Kiadó, Budapest, Hungary 2010

Abstract The eutectoid transformation may be defined as a solid-state diffusion-controlled decomposition process of a high-temperature phase into a two-phase lamellar aggregate behind a migrating boundary on cooling below the eutectoid temperature. In substitutional solid solutions, the eutectoid reaction involves diffusion of the solute atoms either through the matrix or along the boundaries or ledges. The effect of Ag on the non-isothermal kinetics of the reverse eutectoid reaction in the Cu–9 mass%Al, Cu–10 mass%Al, and Cu–11 mass%Al alloys were studied using differential scanning calorimetry (DSC), X-ray diffraction (XRD), and scanning electron microscopy (SEM). The activation energy for this reaction was obtained using the Kissinger and Ozawa methods. The results indicated that Ag additions to Cu–Al alloys interfere on the reverse eutectoid reaction, increasing the activation energy values for the Cu–9 mass%Al and Cu–10 mass%Al alloys and decreasing these values for the Cu–11 mass%Al alloy for additions up to 6 mass%Ag. The changes in the activation energy were attributed to changes in the reaction solute and in Ag solubility due to the increase in Al content.

Keywords Non-isothermal kinetics · Cu–Al alloys · Ag additions · Reverse eutectoid reaction

T. M. Carvalho (✉) · A. T. Adorno · A. G. Magdalena
Departamento de Físico-Química, Instituto de Química-UNESP,
Caixa Postal 355, 14801-970 Araraquara, SP, Brazil
e-mail: thaisamc@iq.unesp.br

R. A. G. Silva
Departamento de Ciências Exatas e da Terra, UNIFESP,
09972-270 Diadema, SP, Brazil

Introduction

The equilibrium solid phases in the Cu-rich corner of the Cu–Al system are the Cu terminal fcc solid solution, designated α and the low-temperature ordered phase based on the fcc structure designated α_2 ; β , the disordered bcc solid solution stable as a high-temperature phase and γ_1 , with structure based on γ brass. The decomposition of the β phase at temperatures below 565 °C involves complex transformations, and a metastable bcc β_1 phase is produced from the β phase by a disorder–order transformation. Subsequently, both β and β_1 decompose into the pearlitic ($\alpha + \gamma_1$) equilibrium structure. A two-phase [$\alpha + \beta$] field exists between the eutectic temperature and the eutectoid reactions $\beta \leftrightarrow (\alpha + \gamma_1)$ at 567 ± 2 °C [1, 2]. The eutectoid transformation is a phase change of the first order, whose rate is dominated by volume or boundary diffusion. The order–disorder transformation occurs as a homogeneous reaction, which may be a nucleation and growth process or a continuous process of atomic interchange [3]. Phases in the Cu–Al–Ag ternary system are structurally analog to those present in the binary systems, without intermediate phases [4, 5].

In this study, the effect of Ag on the non-isothermal kinetics of the reverse eutectoid reaction in the Cu–9 mass%Al, Cu–10 mass%Al, and Cu–11 mass%Al alloys were studied using differential scanning calorimetry (DSC), X-ray diffraction (XRD), and scanning electron microscopy (SEM).

Experimental

The alloys were prepared in an induction furnace under an argon atmosphere, using 99.97% copper, 99.95% aluminum,

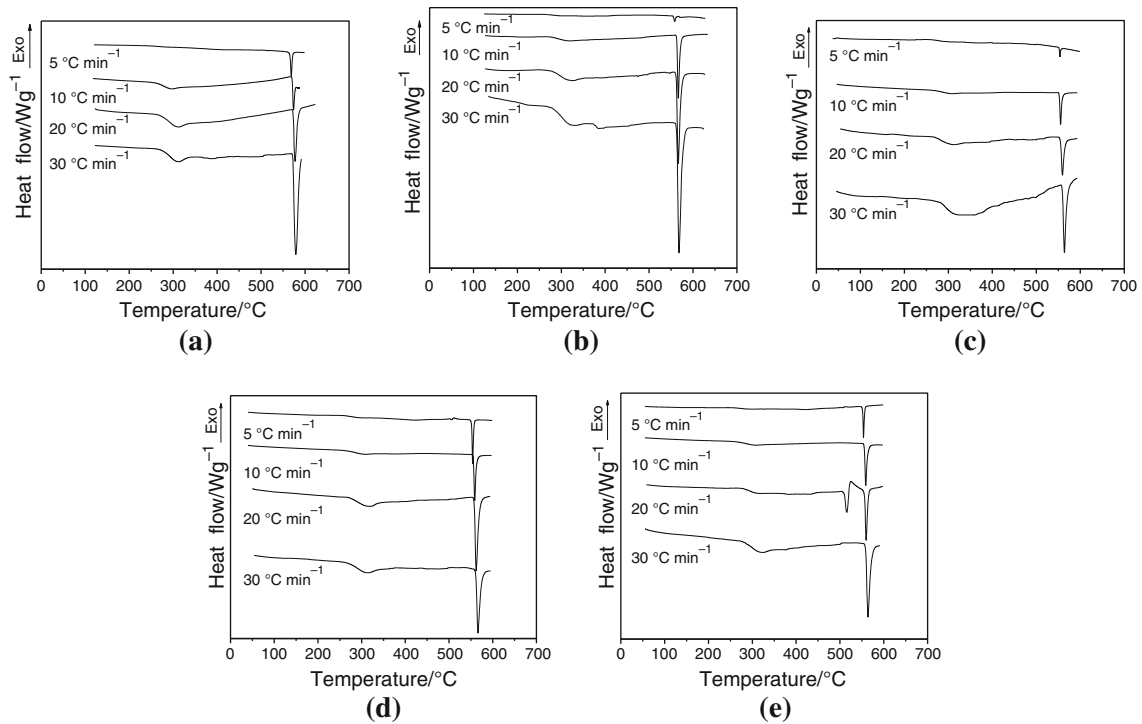


Fig. 1 DSC curves obtained with different heating rates for alloys initially annealed: **a** Cu–9 mass%Al, **b** Cu–9 mass%Al–4 mass%Ag, **c** Cu–9 mass%Al–6 mass%Ag, **d** Cu–9 mass%Al–8 mass%Ag, and **e** Cu–9 mass%Al–10 mass%Ag alloys

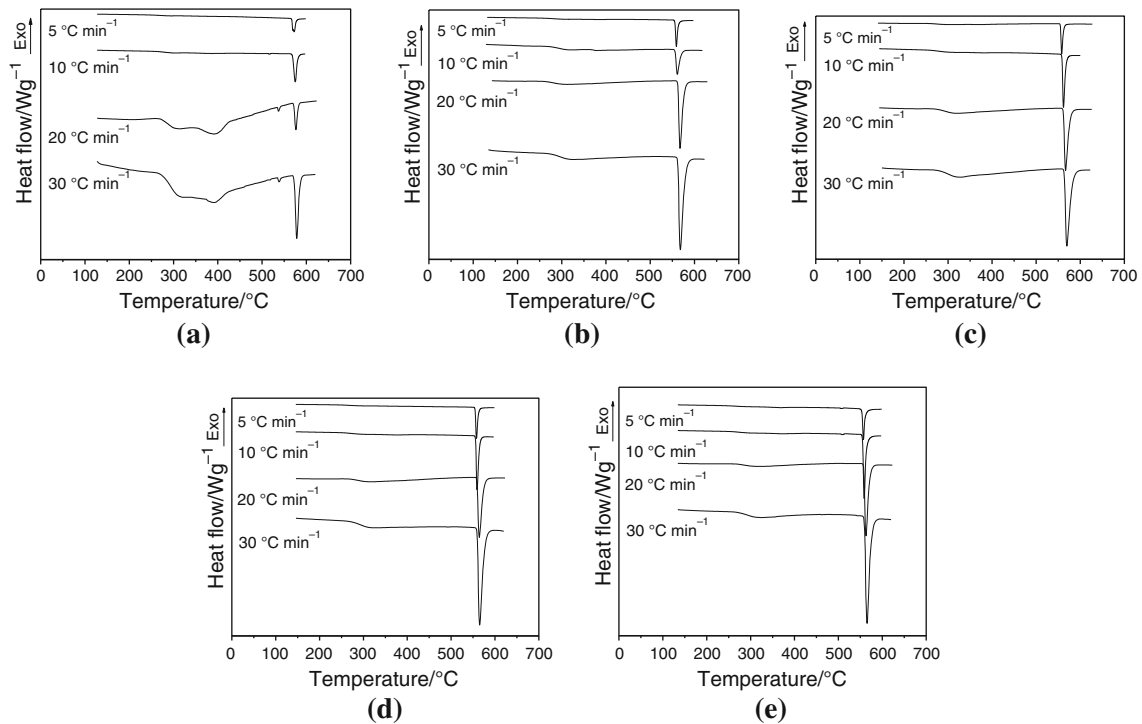


Fig. 2 DSC curves obtained with different heating rates for alloys initially annealed: **a** Cu–10 mass%Al, **b** Cu–10 mass%Al–4 mass%Ag, **c** Cu–10 mass%Al–6 mass%Ag, **d** Cu–10 mass%Al–8 mass%Ag, and **e** Cu–10 mass%Al–10 mass%Ag alloys

and 99.98% silver as starting materials. Results from chemical analysis indicated a final alloy composition very close to the nominal one. Cylindrical samples of 20-mm

diameter and 60-mm length were cut in disks of 2.0-mm thickness. The disks were cold rolled, and flat square samples of 1.0-mm thickness and about 5.0-mm length were

used for SEM and XRD. All samples were annealed during 120 h at 850 °C for homogenization. After the heat treatments, the samples were polished, etched, and examined by SEM using a Jeol JSM T330 electron microscope with a

Noran energy dispersive X-ray (EDX) microanalyzer. The XRD patterns were obtained using a Siemens D5000 4B diffractometer, Cu K α radiation, and solid (not powdered) samples. DSC curves were obtained using a Q20 TA

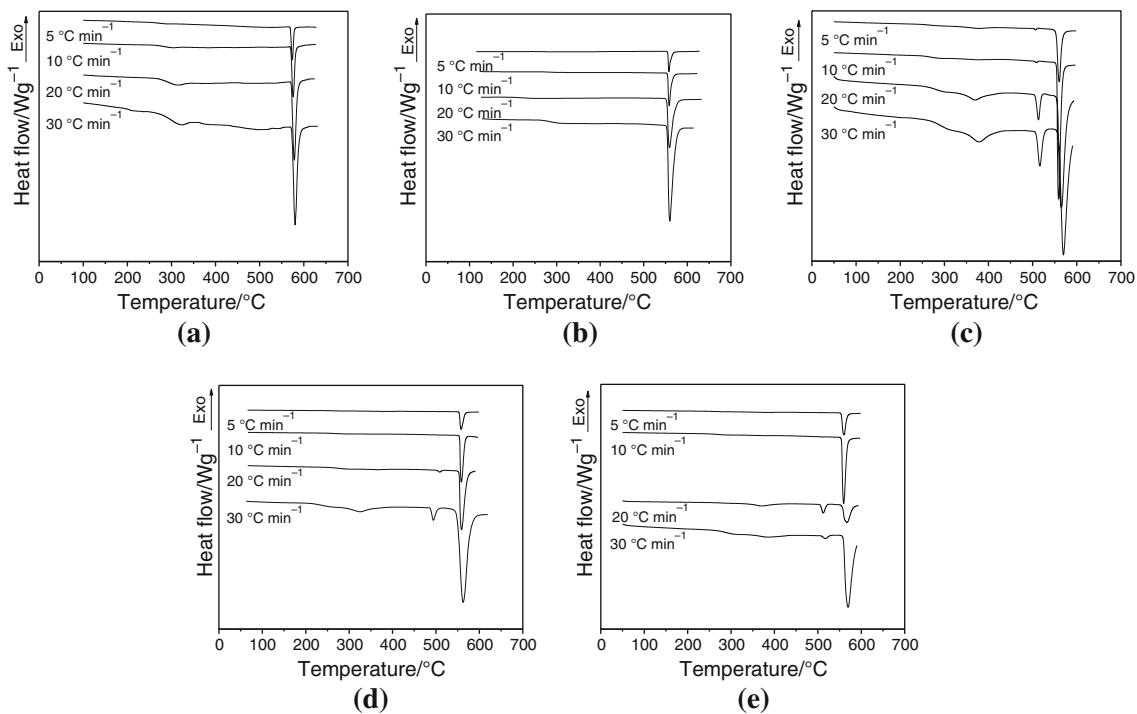


Fig. 3 DSC curves obtained with different heating rates for alloys initially annealed: **a** Cu–11 mass%Al, **b** Cu–11 mass%Al–4 mass%Ag, **c** Cu–11 mass%Al–6 mass%Ag, **d** Cu–11 mass%Al–8 mass%Ag, and **e** Cu–11 mass%Al–10 mass%Ag alloys

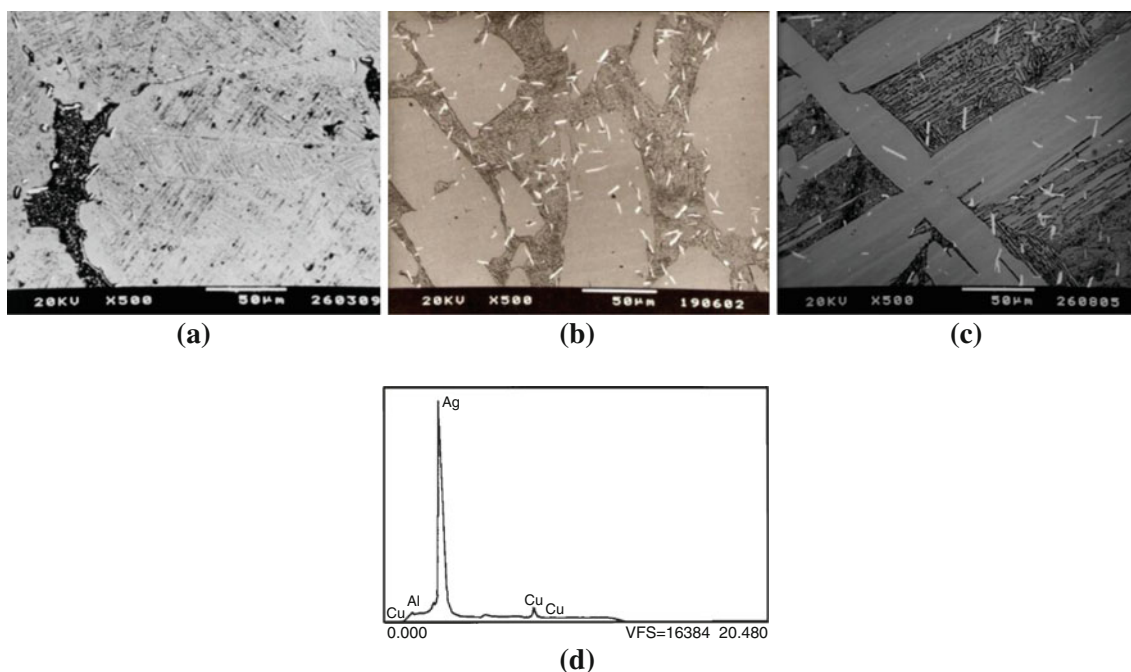


Fig. 4 Scanning electron micrograph obtained for the alloys: **a** Cu–9 mass%Al–6 mass%Ag; **b** Cu–10 mass%Al–6 mass%Ag; **c** Cu–11 mass%Al–6 mass%Ag after annealing and **d** EDX spectrum from the white region on **a**

instrument, aluminum pan, nitrogen flux at about 50 mL min^{-1} and solid samples with 3.0-mm diameter.

Results and discussion

Figures 1, 2 and 3 show the DSC curves obtained at different heating rates for the Cu–9 mass%Al– X mass%Ag alloys, Cu–10 mass%Al– X mass%Ag alloys, and Cu–11 mass%Al– X mass%Ag alloys, where $X = 0, 4, 6, 8,$ and 10 , initially annealed. In Fig. 1a, corresponding to the Cu–9 mass%Al alloy, it is possible to observe two exothermic peaks. The peak at about $300 \text{ }^\circ\text{C}$ is associated with the α_2 disordering reaction, and the peak at about $560 \text{ }^\circ\text{C}$ is attributed to the $(\alpha + \gamma_1) \rightarrow \beta$ reverse eutectoid reaction. These two peaks were observed for all studied alloys, as seen from Figs. 1, 2 and 3. In Figs. 1e, 2a and 3c, d, and e, two additional endothermic peaks were observed. The peak at about $380 \text{ }^\circ\text{C}$ is due to the $(\alpha + \alpha_2) \rightarrow (\alpha + \gamma_1)$ reverse peritectoid reaction, and the peak at about $516 \text{ }^\circ\text{C}$ is associated with the $\beta_1 \rightarrow \beta$ transition. The martensitic phase retained on cooling changes into the β_1 phase in the same temperature interval as the α_2 disordering process and then, at about $516 \text{ }^\circ\text{C}$ the β_1 phase changes into the β phase [6]. These results indicate that the presence of Ag is increasing the martensitic phase fraction retained on cooling.

Figures 4 and 5 show the scanning electron micrographs, the EDX spectrum, and the XRD patterns obtained for annealed alloys and corresponding to the starting point of curves in Figs. 1, 2 and 3. In the micrographs of Fig. 4a, b, c, one may observe the presence of the primary α phase (light) together with the $(\alpha + \gamma_1)$ pearlitic phase (dark) and Ag-rich precipitates (white). This is confirmed by the EDX spectrum in Fig. 4d and the XRD patterns in Fig. 5.

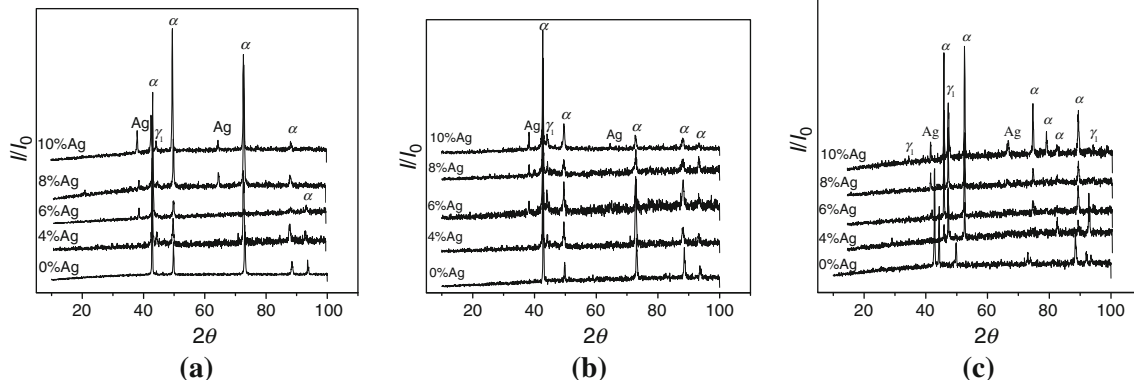


Fig. 5 X-ray diffraction patterns obtained for the annealed alloys: **a** Cu–9 mass%Al– X mass%Ag; **b** Cu–10 mass%Al– X mass%Ag; **c** Cu–11 mass%Al– X mass%Ag

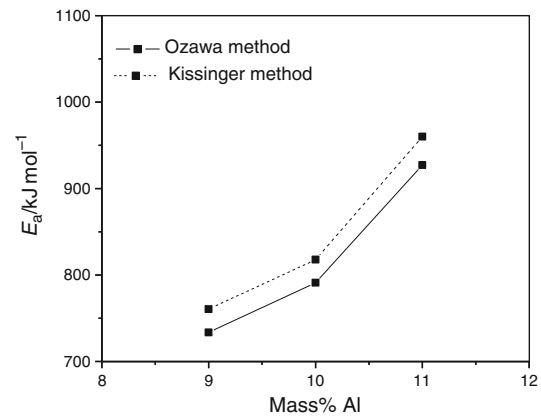


Fig. 6 Plot of activation energy values versus Al concentration, obtained by the Kissinger and Ozawa methods

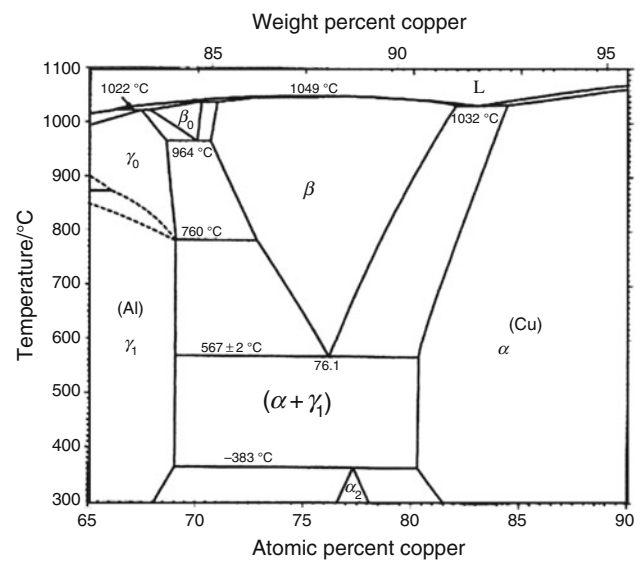


Fig. 7 Cu-rich part of the Cu–Al phase diagram [9]

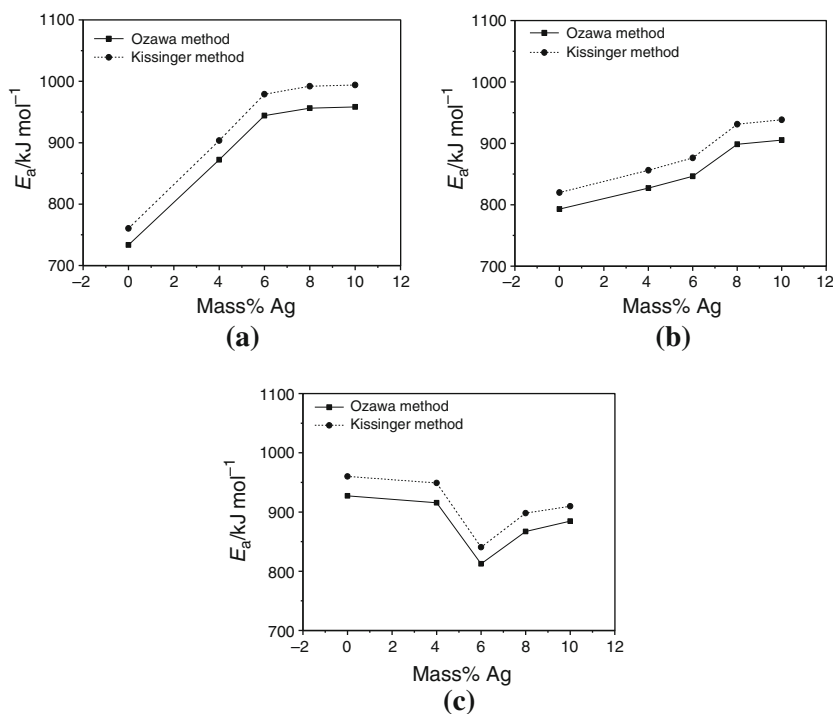
The methods of Kissinger and Ozawa were used to study the influence of additions of 4, 6, 8, and 10 mass%Ag on the activation energy of the $(\alpha + \gamma_1) \rightarrow \beta$ reverse eutectoid reaction in the Cu–9 mass%Al, Cu–10 mass%Al, and Cu–11 mass%Al alloys, considering the last peak in Figs. 1, 2 and 3 and that this reaction is diffusion controlled and only occurs on continuous heating [7]. The activation energy of a transformation, E_a , can be evaluated by measuring the temperature T_m at the point of maximum reaction rate, while heating at a constant rate ϕ . In a DSC experiment, the maxima in reaction rate coincide with the exothermic peak associated with the transformation in the DSC trace. Measuring the peak temperatures at varying heating rates and determining the slope of a plot of either $\ln \phi$ (Ozawa method) or $\ln (\phi/T_m^2)$ (Kissinger method) against $1/T_m$ enables the evaluation of the activation energy [8].

Figures 6 and 8 show, respectively, the plots of activation energy versus Al concentration and activation energy versus Ag concentration obtained for the $(\alpha + \gamma_1) \rightarrow \beta$ reverse eutectoid reaction using the Kissinger and Ozawa methods. In these plots, it is possible to observe that the results obtained by both methods are similar, indicating that these two methods can describe well the considered reaction. It is also observed in these plots an increase in the activation energy values with the increase of Al concentration (Fig. 6) and with the increase in the Ag additions up to 6 mass%Ag for the Cu–9 mass%Al alloy (Fig. 8a) and up to 8 mass%Ag for the Cu–10 mass%Al alloy (Fig. 8b). For the Cu–11 mass%Al alloy (Fig. 8c), the activation

energy values decrease up to 6 mass%Ag and then increase with the increase of Ag content.

The results indicated that Ag additions to Cu–Al alloys interfere on the reverse eutectoid reaction, increasing the activation energy values for the Cu–9 mass%Al and Cu–10 mass%Al alloys and decreasing these values for the Cu–11 mass%Al alloy for additions up to 6 mass%Ag. These changes in the activation energy may be ascribed to the Al–Ag interaction on the Cu–Al matrix. At temperatures higher than 560 °C, the studied alloys are in the hypoeutectoid $[\alpha + \beta]$ field, as may observed from the Cu–Al phase diagram[9] (Fig. 7), and part of Ag is dissolved in the α phase and other part in the β phase. The primary Cu-rich α phase of Cu–Al–Ag alloys is a fcc solid solution of Al and Ag in copper and the copper–silver miscibility gap in the Cu–Ag system results from the excessive disparity between Cu and Ag atoms (large size factor) while the Ag–Al system is an example of a very small size factor[4]. So, Ag solubility may be larger at higher Al content and, for the Cu–9 mass%Al and Cu–10 mass%Al alloys the increase in Ag concentration will increase the Al relative fraction which is able to react with Cu to produce the β phase. The increase in the Al relative fraction will correspond to a decrease in the Cu relative fraction which participates in the reaction, thus increasing the activation energy. For the Cu–11 mass%Al alloy with Ag additions, the increase in the Al concentration will shift the equilibrium concentration to values close to that of the eutectoid point and now the β phase formation reaction will

Fig. 8 Plots of activation energy changes versus Ag concentration: **a** Cu–9 mass%Al– X mass%Ag ($X = 0, 4, 6, 8,$ and 10); **b** Cu–10 mass%Al– X mass%Ag ($X = 0, 4, 6, 8,$ and 10); **c** Cu–11 mass%Al– X mass%Ag ($X = 0, 4, 6, 8,$ and 10) alloys



occur with Al as the solvent, instead of Cu, and the increase in the Al content will now decrease the activation energy for the reaction. From Fig. 8, it is possible to observe that Ag additions are more effective for lower Ag concentrations. This may be related to changes in Ag solubility with Al concentration and the results indicate that the Ag solubility limit in the studied alloys is between 6 and 8 mass%. The decrease in the activation energy values with the increase in the Al content for Cu–Al hypereutectoid alloys may be confirmed by the result obtained by Kwarciak [3], who found $E_a = 650 \text{ kJ mol}^{-1}$ for the Cu–12.4 mass%Al alloy.

Conclusions

The results indicated that Ag additions to Cu–Al alloys interfere on the reverse eutectoid reaction, increasing the activation energy values for the Cu–9 mass%Al and Cu–10 mass%Al alloys and decreasing these values for the Cu–11 mass%Al alloy for additions up to 6 mass%Ag. The changes in the activation energy were attributed to changes in the reaction solute and in Ag solubility due to the increase in Al content.

Acknowledgements The authors thank the support of FAPESP (Project no. 2006/04718-0) and Capes.

References

1. Massalski TB. Binary alloy phase diagrams. 2nd ed. Ohio: American Society for Metals; 1992.
2. Kulkarni SD. Thermodynamics of martensitic and eutectoid transformations in the Cu–Al system. Thermodynamique des transformations martensitique et eutectoide dans le systeme Cu–Al Thermodynamik martensitischer und eutektoider umwandlungen im system Cu–Al. Acta Metall. 1973;21(10):1461–9.
3. Kwarciak J. Kinetics of phase transformations in Cu–Al and Cu–Zn–Al alloys. J Therm Anal. 1986;31:1279–87.
4. Massalski TB, Perepezko JH. Constitution and phase relationships in copper–silver–aluminum ternary-system. Z. Metallkd. 1973;64: 176–81.
5. Adorno AT, Cilense M, Garlipp W. Phase relationships in the Cu–Ag–Al ternary system near the copper-rich corner. J Mater Sci Lett. 1989;8:1294–7.
6. Adorno AT, Silva RAG. Phase transformations in the Cu–Al alloy with Ag addition. J Therm Anal Calorim. 2005;79:445–9.
7. Adorno AT, Silva RAG, Carvalho TM. ($\alpha + \gamma_1$) Complex phase formation in the Cu–10 mass% Al–6 mass% Ag alloy. J Therm Anal Calorim. 2009;97:127–30.
8. Baram J, Erukhimovitch V. Application of thermal analysis methods to nucleation and growth transformation kinetics. Thermochim Acta. 1997;29:81–4.
9. Murray JL. The aluminium–copper system. Int Met Rev. 1985;30: 211–33.